Fine structure characterization of zero-valent iron nanoparticles for decontamination of nitrites and nitrates in wastewater and groundwater



2008 Sci. Technol. Adv. Mater. 9 025015

(http://iopscience.iop.org/1468-6996/9/2/025015)

IOP PUBLISHING SCIENCE AND TECHNOLOGY OF ADVANCED MATERIALS

Sci. Technol. Adv. Mater. **9** (2008) 025015 (9pp) doi:10.1088/1468-6996/9/2/025015

# Fine structure characterization of zero-valent iron nanoparticles for decontamination of nitrites and nitrates in wastewater and groundwater

**Kuen-Song Lin[1], Ni-Bin Chang[2] and Tien-Deng Chuang[1]**

[1] Department of Chemical Engineering & Materials Science/Fuel Cell Center, Yuan Ze University, Chung-Li City 320, Taiwan, Republic of China
[2] Civil and Environmental Engineering Department, University of Central Florida, Orlando, FL 32816, USA

E-mail: kslin@saturn.yzu.edu.tw

Received 24 November 2007
Accepted for publication 19 February 2008
Published 24 July 2008
Online at stacks.iop.org/STAM/9/025015

**Abstract**

The main objectives of the present study were to investigate the chemical reduction of nitrate or nitrite species by zero-valent iron nanoparticle (ZVIN) in aqueous solution and related reaction kinetics or mechanisms using fine structure characterization. This work also exemplifies the utilization of field emission-scanning electron microscope (FE–SEM), transmission electron microscopy (TEM), and x-ray diffraction (XRD) to reveal the speciation and possible reaction pathway in a very complex adsorption and redox reaction process. Experimentally, ZVIN of this study was prepared by sodium borohydride reduction method at room temperature and ambient pressure. The morphology of as-synthesized ZVIN shows that the nearly ball and ultrafine particles ranged of 20–50 nm were observed with FE–SEM or TEM analysis. The kinetic model of nitrites or nitrates reductive reaction by ZVIN is proposed as a pseudo first-order kinetic equation. The nitrite and nitrate removal efficiencies using ZVIN were found 65–83% and 51–68%, respectively, based on three different initial concentrations. Based on the XRD pattern analyses, it is found that the quantitative relationship between nitrite and Fe(III) or Fe(II) is similar to the one between nitrate and Fe(III) in the ZVIN study. The possible reason is due to the faster nitrite reduction by ZVIN. In fact, the occurrence of the relative faster nitrite reductive reaction suggested that the passivation of the ZVIN have a significant contribution to iron corrosion. The extended x-ray absorption fine structure (EXAFS) or x-ray absorption near edge structure (XANES) spectra show that the nitrites or nitrates reduce to $N_2$ or $NH_3$ while oxidizing the ZVIN to $Fe_2O_3$ or $Fe_3O_4$ electrochemically. It is also very clear that decontamination of nitrate or nitrite species in groundwater via the *in-situ* remediation with a ZVIN permeable reactive barrier would be environmentally attractive.

Keywords: zero-valent iron nanoparticles, nitrite, nitrate, chemical reduction, kinetics, XANES/EXAFS

 

## 1. Introduction

In recent years, the emergence of nitrite ($NO_2^-$) and nitrate ($NO_3^-$) contaminants in wastewater and groundwater has become a serious concern in many countries. In Taiwan, nitrite or nitrate levels in wastewater effluent are around 10–500 mg $l^{-1}$ depending on the sources. The range of nitrite or nitrate concentrations in groundwater varies from 1 to 150 mg $l^{-1}$, depending on the types of local impacts, such as agricultural runoff, leaching after the application of fertilizers, intensive operations of animal feeding, food processing, and industrial waste discharge. Such contamination may place drinking water quality at risk and endanger the public health. While nitrate or nitrite species are known to be toxic and carcinogenic, site remediation becomes necessary in order to reduce the impacts on human health, such as methemoglobinemia, cancer and damage to liver, and improve the ecosystem integrity [1–3]. Thus, the regulatory standards of nitrite and nitrate of Environmental Protection Administration (EPA) in Taiwan for groundwater and wastewater were being set up at 1–10 and 10–100 mg $l^{-1}$ depending on the category of sources, respectively. Recently, to ensure safe drinking water quality in Taiwan, the regulatory standards of nitrite and nitrate were being set up at 0.1 and 10 mg $l^{-1}$, respectively [4].

The removal of nitrite and nitrate from contaminated wastewater frequently involves microbial nitrification/denitrification, ion exchange, reverse osmosis, electrocatalytic, and high temperature and chemical reduction process [5–10]. Microbial reactions are inefficient due to generally slow process and required intensive maintenance, including the constant supply of organic substances as electron donors. Nitrate species cannot be destroyed efficiently by ion exchange and reverse osmosis processes either. Electrocatalytic process requires higher potential for reduction of nitrite ion to nitrogen species for most electrodes surfaces. Furthermore, higher installation and maintenance costs with the complexity of regeneration of membrane and brine disposal significantly constrain the use of reverse osmosis process. Chemical reduction process might be relatively efficient for denitrification process [8–12]. Reduction of nitrite/nitrate using ZVIN is deemed the most cost-effective option in many studies [13–15]. Therefore, innovative applications of the ZVIN for in-situ groundwater remediation or for the treatment of industrial waste streams contaminated with redox active toxic material can often be found [16–19]. However, the reaction mechanism of nitrite/nitrate removals is significantly dependent on pH, both in buffered and unbuffered solutions [13–15]. The ZVIN is considered as a suitable source of electrons and could potentially stabilize several elements in contaminated soil and groundwater systems because its oxidation would only cause minor changes in pH.

There is a renewed interest of applying a suit of instruments for promoting the understanding of material property of the ZVIN in environmental engineering and science regime. First of all, TEM is an imaging technique whereby a beam of electrons is transmitted through a specimen leading to form an image. The image is then magnified and directed to appear either on a fluorescent screen or layer of photographic film, or to be detected by a sensor to describe the ZVIN surfaces. XRD is a versatile, non-destructive technique that reveals detailed information about the chemical composition and crystallographic structure of the ZVIN. On the other hand, FE-SEM technique has limited detection sensitivity and resolution to identify the chemical structures of the ZVIN surfaces. However, when x-rays pass through any sort of material, a proportion of them are absorbed in the sense that measuring the amount of absorption with increasing x-ray energy reveals so-called edge structures, where the level of absorption suddenly increases. Analysis of these XANES oscillations in the spectrum of a particular sample can provide information about vacant orbitals, electronic configuration and the site symmetry of the absorbing atom. Thus, the x-ray absorption spectroscopy offers the basic knowledge of understanding the oxidation states and fine structures of Fe atoms in the ZVIN contributing to an advanced study of the chemical reduction effect of nitrite or nitrate contaminants in wastewater or groundwater [20, 21]. It uniquely provides the information of electronic configuration, stereochemistry and the oxidation states of the metallic Fe atoms in the ZVIN [21–23]. In addition, EXAFS spectroscopy can also investigate the information on the Fe atomic arrangement of the ZVIN in terms of bond distance, number and kind of near neighbors, thermal and static disorder [20–23]. On the contrary, XRD or SEM/EDS technique has not enough detection sensitivity and resolution for this purpose.

Given that the mechanism of the chemical reduction of nitrite or nitrate contaminants on the surface of the ZVIN still remains unclear, the main objectives of the present study were to investigate the kinetics for illuminating the chemical reduction mechanism of nitrite or nitrate contaminants on the surface of the ZVIN and the fine structures and oxidation states of the fresh or used ZVIN by using XRD, FE-SEM, TEM, XANES and EXAFS techniques. The surface reductive reaction mechanisms and pathways of nitrate and nitrite contaminants on the ZVIN were also discussed for improving the application potential in groundwater remediation. Finally, the hypothesis of a pseudo-first order reaction for nitrite and/or nitrate removal with the ZVIN was assumed that would be expected to have a good agreement with several previous studies [10, 16, 18].

## 2. Experimental

### *2.1. Preparation of the ZVIN*

In the present work, the ZVINs were tested for their ability to reduce and remove $NO_2^-$ and $NO_3^-$ from groundwater or waste streams. The ZVINs were prepared by the reduction of an aqueous iron salt using an easy-controlled and effective reductant of sodium borohydride ($NaBH_4$). About 10 g of $FeSO_4$ $7H_2O$ were dissolved in 100 ml of 30% ethanol and 70% deionized water. The pH value was adjusted to about 6.8 with 3.8 N $NaOH_{(aq)}$. About 1.8 g of $NaBH_4$ powder were

added incrementally to the mixture, allowing the forming to subside between increments. After the addition of the $NaBH_4$ powder, the mixture was stirred for about 20 min and then filtered through a 0.22 $\mu$m filter. Just prior to the formation of a liquid meniscus between the ZVIN, the solid residues were washed several times with ethanol, effectively substituting ethanol solutions for the water in the mixture. The step could help to prevent immediate rusting as the filtration process had been completed. The resulting ZVINs were vacuum-dried overnight.

### *2.2. Characterization of ZVIN*

The physical data of pore volume (or geometrically-defined pore size distribution) and specific surface area of the ZVIN were obtained from the conventional analysis of nitrogen isotherms measured by nitrogen adsorption (Micromeritics ASAP 2010 Instrument) at 77 K. These data were basically calculated using Barrett–Joyner–Halenda (BJH) method of adsorption isotherms (based on the Kelvin equation) and BET (Brunauer, Emmett, and Teller) equation, respectively [24]. All the samples were degassed at 100 °C prior to the measurement. Crystalline structures of the ZVIN were measured by XRD scanned from 10° to 80° ($2\theta$) with a scan rate of $4^\circ(2\theta)\,\mathrm{min}^{-1}$ with monochromatic CuK$\alpha$ radiation (MAC Science, MXP18). The morphology of the ZVIN was determined by FE-SEM/EDS (Hitachi, S-4700 Type II). TEM (Hitachi H-7500) analyses were conducted to investigate the particle size distribution and microstructures, using 120 kV accelerating voltage, with a resolution of 0.1 nm. EXAFS and XANES spectra were both collected at the Wiggler beamline BL 17C1 at the National Synchrotron Radiation Research Center (NSRRC) of Taiwan. The electron storage ring was operated with energy of 1.5 GeV and a current ranged of 100–200 mA. A Si(111) DCM was used for providing highly monochromatized photon beams with energies of 5 to 15 keV and resolving power (E/$\Delta$E) of up to 7000. Data were collected in fluorescence or transmission mode with a Lytle ionization detector [22] for Fe (7112 eV) K edge experiments at room temperature. The $k^2$- or $k^3$-weighted and EXAFS spectra were Fourier transformed to $R$ space over the range between 2.5 and 12.5 $\mathrm{Å}^{-1}$. The EXAFS data were analyzed by the UWXAFS 3.0 program and FEFF 8.0 codes [20–23].

### *2.3. Kinetics of nitrite/nitrate degradation on the ZVIN*

$NaNO_2$ and $KNO_3$ of reagent grade were selected as the target compounds ($NO_2^-$ and $NO_3^-$) respectively in this study for the chemical reduction on the ZVIN. Three different concentrations of 150, 200, and 250 $\mathrm{mg\,l}^{-1}$ for $NO_2^-$ and $NO_3^-$ contaminants in aqueous solution were prepared by dissolving desired quantities of $NaNO_2$ and $KNO_3$ in the high-purity de-ionized water. Rate constants of kinetic studies were determined by adding the freshly prepared ZVIN at a concentration of $5\,\mathrm{g\,l}^{-1}$ to 400 ml generating different concentrations of $NO_2^-$ or $NO_3^-$ solutions in 500 ml glass beakers for each set of experiments. Chemical reduction of nitrate/nitrate by the ZVIN at ambient temperature, and the desired testing with respect to varying $NO_2^-$ or $NO_3^-$ concentrations were simultaneously conducted in various glass beakers using a jar test apparatus at a mixing rate of 200 rpm. In each set of experiments the reaction vessels were removed one by one from the jar test apparatus at intervals of 10–60 min during the 240-min reaction. Liquid samples were taken by a syringe every 10, 20, 30 or 60 min for about 4 h and filtered through a 0.22 $\mu$m PVDF syringe filter. Concentrations of nitrate, nitrite or ammonium ($NH_4^+$) species were both determined by ion chromatography (IC, Dionex ICS-1000) and OIA FIA/SFA (Model FS-3100). The gaseous product $N_2$ generated in the chemical reduction process of $NO_2^-$ or $NO_3^-$ solutions on the ZVIN were detected GC/TCD (Aligent Model 6890N with TCD).

## 3. Results and discussion

### *3.1. Morphology and crystalline structure of ZVIN*

The reaction mechanism for nitrate removal by the ZVIN may appear to be a surface precipitation or complexation of nitrate or nitrite with the ZVIN. The ZVIN have a surface area of $43\,\mathrm{m^2\,g^{-1}}$ while bulk Fe(0) particles have a surface area of $0.5\,\mathrm{m^2\,g^{-1}}$ measured by Brunauer, Emmett and Teller (BET) adsorption isotherms [24]. Therefore, the ZVIN was more efficient than bulk ones for the remediation of nitrate/nitrite-contaminated groundwater. In addition, the ZVIN led to a higher oxidative fraction on particle surface compared to bulk ones. It indicates that the complete and active oxidation on the surface of the ZVIN might enable the potential use of the ZVIN because their surface-to-volume ratio is very high.

The morphology of the different iron surfaces and measurement the particle sizes were analyzed by using FE-SEM (figures 1(a) and (b)) and TEM (figures 1(c) and (d)). The ZVIN in figures 1(a) and (c) exhibited nearly ball and ultrafine particles, represented that the ZVIN ranged of 20–50 nm. Since the strong magnetic forces on the ZVIN, the nanoparticles were not all separated and the sizes were narrowly distributed with a cluster structure formed, which are clearly represented by the TEM or FE-SEM images. On the other hand, figures 1(b) and (d) show that the ZVIN were oxidized and cracked, relative to the figures 1(a) and (c) which were on the order of 10–30 nm in size. This change was due to the aggregation of Fe(III) nanoparticles (i.e. $Fe_2O_3$) on the surface of the ZVIN, thus the magnetic force has revealed. Therefore, used ZVIN are distributed well enough, even though magnetic properties are involved from the inner core fairly.

The XRD pattern (figure 2(a)) shows that the Fe(0) standard characteristic peaks of $2\theta = 44.59$ and 64.62, which indicates that the crystallization of the ZVIN. The ZVIN having the smaller particle sizes and lower crystal structure shows a relatively broad peak. The diffraction patterns of the ZVIN show that all the Fe(0) nanoparticles were single-phase cubic closest-packed structure. As shown in figure 2(b), the pre-edge XANES spectra of the fresh ZVIN might exhibit an absorbance feature. The fine structural parameter of the fresh ZVIN catalyst indicates the Fe atom is in the formation

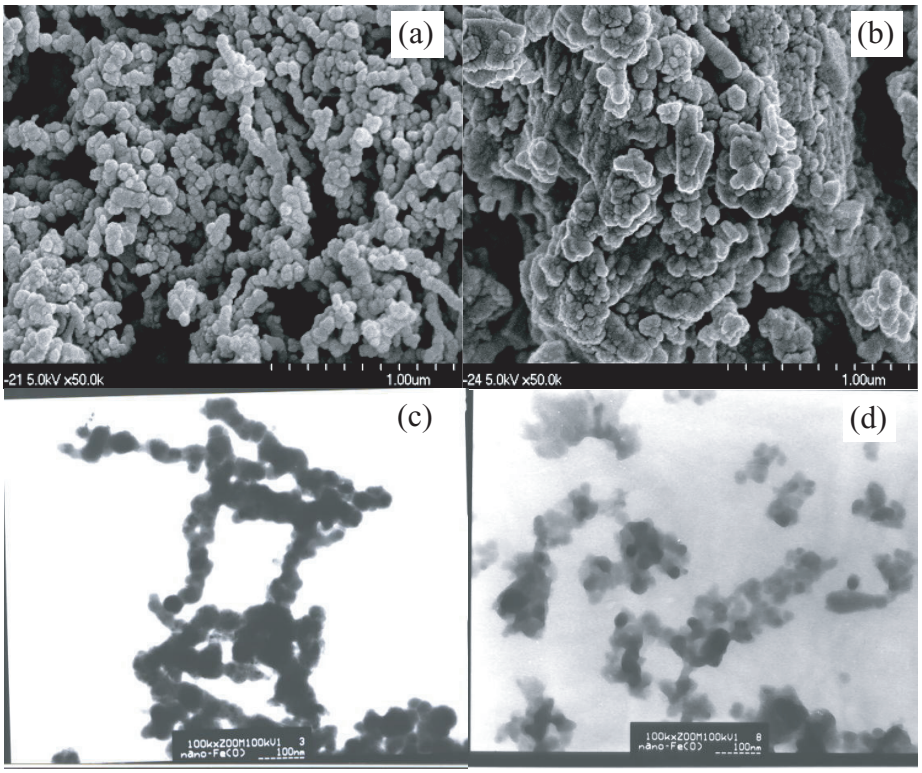


**Figure 1.** FE-SEM microphotos and TEM images of (a), (c) fresh and (b), (d) used ZVIN, respectively, for the chemical reduction of nitrite or nitrate solutions.

of Fe–Fe with bond distances 2.25 Å and the corresponding coordination number (CN) is 9.66 for the first shell of central Fe atom confirmatively. Standard deviation calculated from the averaged spectra was also determined. In all EXAFS data analyzed, the Debye–Waller factors ($\Delta\sigma^2$) were less than 0.024 (Å$^2$).

### *3.2. Kinetics analyses*

Kinetics studies has significant role for the design of a proper rector to produce the desired product. The ZVIN corrosion is primarily occurred due to the formation of Fe(II) or mainly Fe(III) species. Nitrate/nitrite reduction via the formation of nitrogen by using the ZVIN [8–12] can be described as:

$$\mathrm{Fe^0 \rightarrow Fe^{2+} + 2e^-} \quad (E_0 = -0.44\ \mathrm{eV}), \tag{1}$$

$$\mathrm{Fe^{2+} \rightarrow Fe^{3+} + e^-} \quad (E_0 = 0.77\ \mathrm{eV}), \tag{2}$$

$$\mathrm{Fe^0 \rightarrow Fe^{3+} + 3e^-} \quad (E_0 = 0.33\ \mathrm{eV}), \tag{3}$$

$$\mathrm{Fe^0 + 2NO_2^- + 8H^+ + 3e^- \rightarrow Fe^{3+} + 4H_2O + N_2} \quad (E_0 = 1.85\ \mathrm{eV}), \tag{4}$$

$$\mathrm{Fe^0 + 2NO_2^- + 8H^+ + 4e^- \rightarrow Fe^{2+} + 4H_2O + N_2} \quad (E_0 = 1.08\ \mathrm{eV}), \tag{5}$$

$$\mathrm{Fe^0 + 2NO_3^- + 12H^+ + 7e^- \rightarrow Fe^{3+} + 4H_2O + N_2} \quad (E_0 = 1.57\ \mathrm{eV}), \tag{6}$$

$$\mathrm{Fe^0 + 2NO_3^- + 12H^+ + 8e^- \rightarrow Fe^{2+} + 4H_2O + N_2} \quad (E_0 = 0.8\ \mathrm{eV}), \tag{7}$$

$$\mathrm{Fe^0 + 2NO_2^- + 16H^+ + 9e^- \rightarrow Fe^{3+} + 4H_2O + 2NH_4^+} \quad (E_0 = 2.124\ \mathrm{eV}), \tag{8}$$

$$\mathrm{Fe^0 + 2NO_2^- + 16H^+ + 10e^- \rightarrow Fe^{2+} + 4H_2O + 2NH_4^+} \quad (E_0 = 1.354\ \mathrm{eV}), \tag{9}$$

$$\mathrm{Fe^0 + 2NO_3^- + 20H^+ + 13e^- \rightarrow Fe^{3+} + 4H_2O + 2NH_4^+} \quad (E_0 = 1.844\ \mathrm{eV}), \tag{10}$$

$$\mathrm{Fe^0 + 2NO_3^- + 20H^+ + 14e^- \rightarrow Fe^{2+} + 4H_2O + 2NH_4^+} \quad (E_0 = 1.074\ \mathrm{eV}). \tag{11}$$

It is evident that both nitrogen gas and ammonium are possibly to be formed in the reaction with ZVIN. The pathway

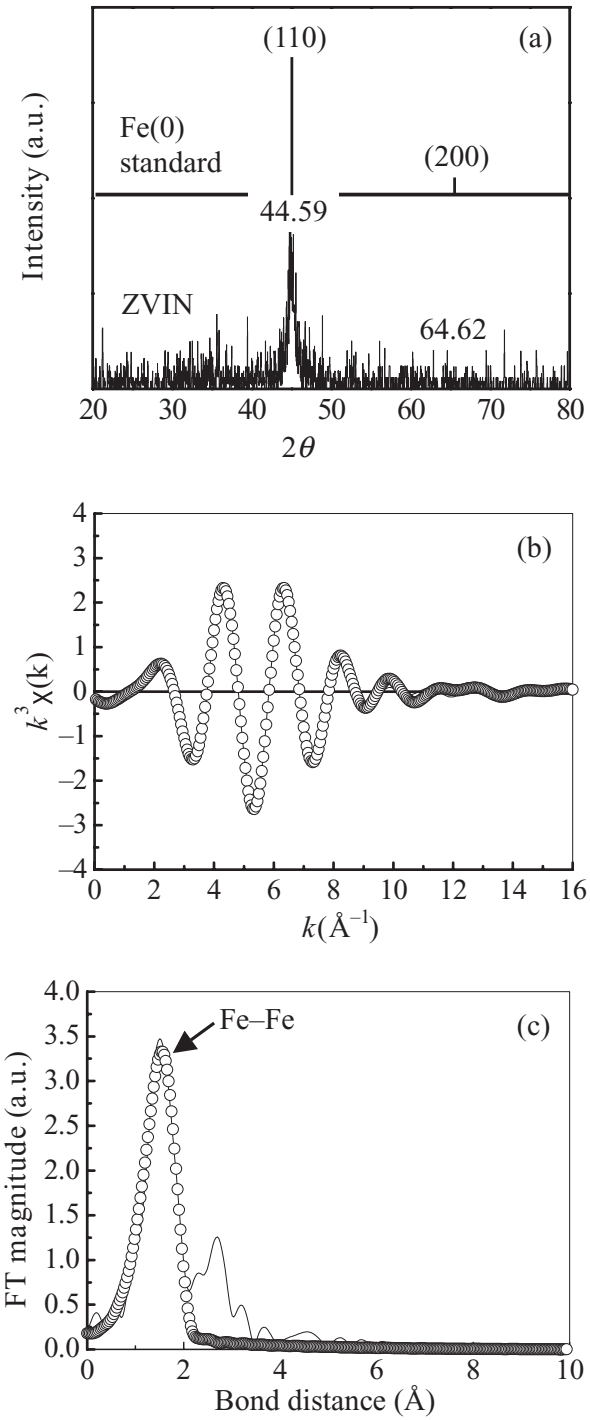


**Figure 2.** (a) XRD pattern (characteristic peaks of $2\theta$ = 44.59 and 64.62), (b) Fe K-edge EXAFS oscillation $k^3 \times (k)$, and (c) Fourier transform (FT) of EXAFS $k^3 \times (k)$ of the fresh ZVIN. The best fitting of the EXAFS spectra are expressed with the circle lines.

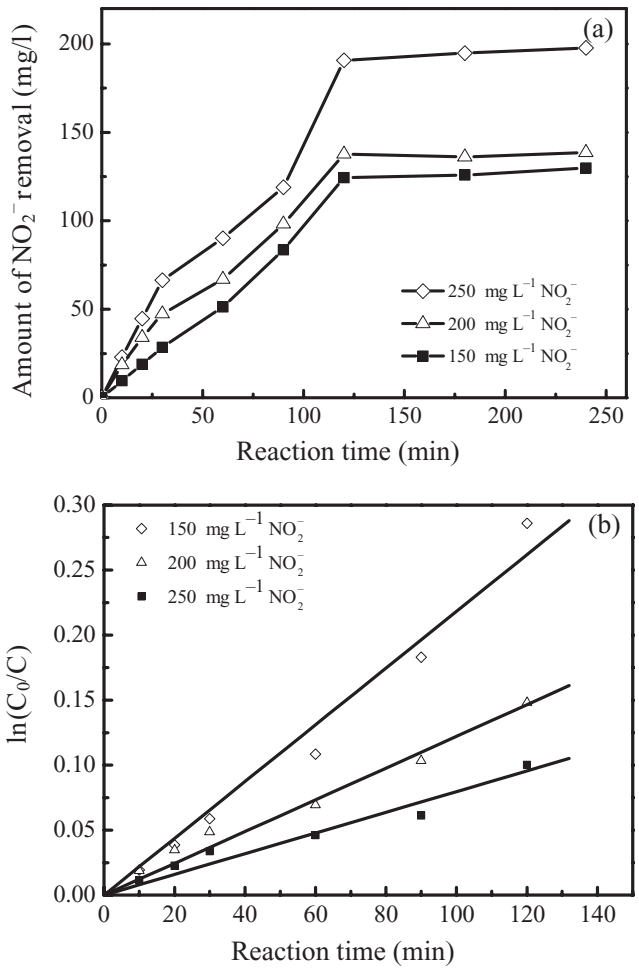


**Figure 3.** Reductive kinetics of (a) $NO_2^-$ removal as a function of reaction time in the presence of ZVIN and (b) a plot of $\ln(C_0/C)$ versus reaction time (min). The initial concentrations of nitrite solution were 150, 200, and 250 mg $l^{-1}$. The metal/solution ratio and the mean resulting $R^2$ value were 5 g ZVIN $L^{-1}$ and 0.9823, respectively.

of ammonium production is even more thermodynamically active when comparing equations (6) and (10) or equations (4) and (8). According to equations (8)–(11), if the pH value is low, the formation of ammonia would be much more frequent on the ZVIN surfaces. Nitrite readily reduces with two or three moles ZVIN and oxidizes one mole Fe(III) and three moles Fe(II) and where as, six or two moles nitrates reduce to oxidize five moles Fe(III) and Fe(II). Therefore, the results from the figures 3(a) and 4(a) represents that nitrites and nitrates reduction corresponds to the rate proportional to the disappearance of nitrate/nitrite concentration [C] as follows:

$$-\mathrm{d}C/\mathrm{d}t = k[C]^{\mathrm{m}}[\mathrm{Fe}]^{\mathrm{n}}, \quad -\mathrm{d}C/\mathrm{d}t = k[C]^{\mathrm{m}},$$

where solid concentration of the ZVIN were considered as a constant (5 g $l^{-1}$) for each experiment respectively, reaction order ($m$) is assumed as a pseudo first-order, and rate constant $k$ ($\mathrm{min}^{-1}$) is calculated from the slope of the line for $\ln[C_0/C]$ vs. reaction time. Integration of equation results in

$$-\mathrm{d}C/\mathrm{d}t = k[C]^{\mathrm{m}}, \quad \ln[C_0/C] = kt,$$

where, $C_0$ is the initial concentration of dissolved contaminant. The initial concentrations of nitrite or nitrate solutions were 150, 200, and 250 mg $l^{-1}$ respectively. Nitrites or nitrates were declined fast in the beginning up to 120 min but no more reduction has taken place after that. The nitrite and nitrate removal efficiencies were found 65–83 to 51–68%, respectively, with respect to different

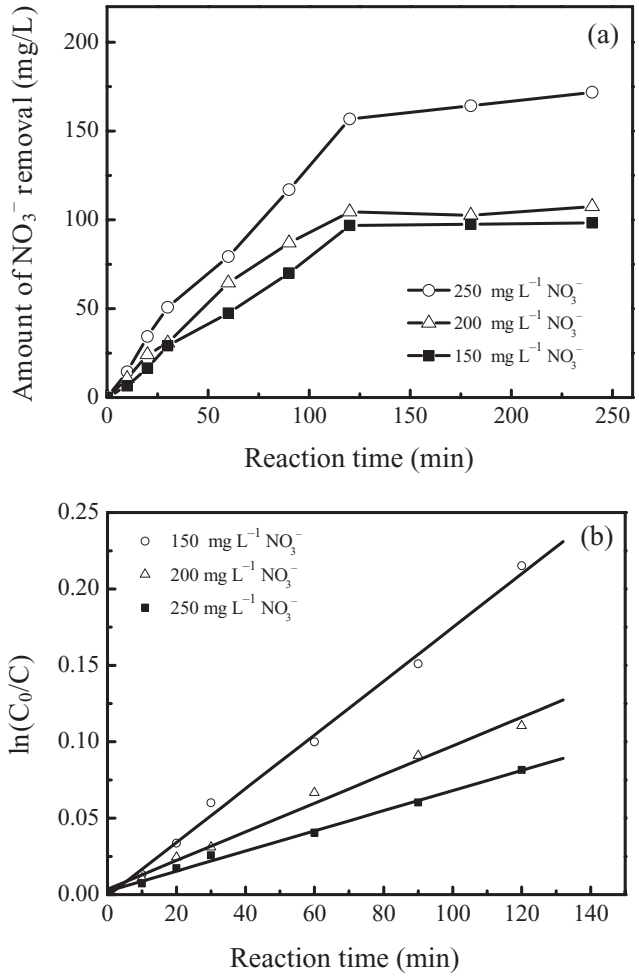


**Figure 4.** Reductive kinetics of (a) $NO_3^-$ removal as a function of reaction time in the presence of ZVIN and (b) a plot of $\ln(C_0/C)$ versus reaction time (min). The initial concentrations of nitrate solution were 150, 200, and 250 mg $l^{-1}$. The metal/solution ratio and the mean resulting $R^2$ value were 5 g ZVIN $L^{-1}$ and 0.9932, respectively.

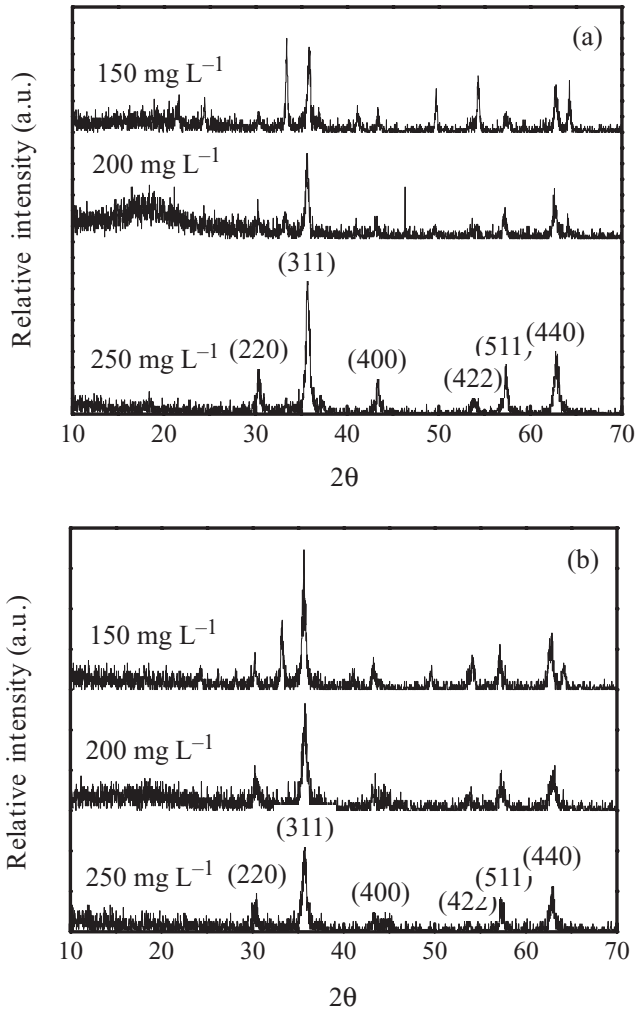


**Figure 5.** XRD patterns of ZVIN for the reduction of (a) $NO_2^-$ and (b) $NO_3^-$ solutions with the initial concentrations of 150, 200, and 250 mg $l^{-1}$, respectively.

concentrations. Increasing the nitrite or nitrate concentration elevates the passivation of ZVIN due to the formation of Fe(II) or Fe(III) [12–19]. Observed reaction order varies with different initial nitrate and nitrite concentrations. Included in the table 1 with rate constants may be a good support of this observation. Rates of the reaction orders have been calculated from liner regression of $\ln[C_0/C]$ vs. reaction time for the reduction of nitrites and nitrates are 0.9823 and 0.9932, respectively represents in the figures 3(b) and 4(b). Hence, a pseudo-first order reaction rate for nitrite or nitrate removal with the ZVIN may eventually be confirmed in this paper. The $R^2$ values are slightly lower with respect to differing nitrites than nitrates concentrations. The reduction rate of nitrites is relatively higher removal than that of nitrates with regard to their thermodynamic activity.

**Table 1.** Reaction rate equations for chemical reduction of nitrites or nitrates with different initial concentrations by using the ZVIN [d].

| $C_0$ [a] (mg $l^{-1}$) | $m$ [b] | $k$ ($min^{-1}$)[c] | $R^2$ value |
|---|---|---|---|
| Nitrite ($NO_2^-$) (mg $l^{-1}$) | | | |
| 150 | 0.86 | 0.0229 | 0.9875 |
| 200 | 0.91 | 0.0114 | 0.9823 |
| 250 | 0.95 | 0.0075 | 0.9784 |
| Nitrate ($NO_3^-$) (mg $l^{-1}$) | | | |
| 150 | 0.80 | 0.0176 | 0.9954 |
| 200 | 0.87 | 0.0093 | 0.9946 |
| 250 | 0.90 | 0.0066 | 0.9895 |

[a]$C_0$: The initial concentration of nitrite or nitrate solution.
[b]$m$: Reaction order.
[c]$k$: Reaction rate constant.
[d]The metal/solution ratio was 5 g ZVIN $l^{-1}$.

### *3.3. Mechanisms and surface reaction on ZVIN*

In the context of previous studies, the ZVIN could significantly enhance the reduction of nitrite or nitrate on the surface of iron oxides. The XRD patterns (figures 5(a) and (b)) indicate that the amorphous iron oxides are rapidly formed with elevated nitrite or nitrate concentrations. In figure 2(a), the diffraction patterns of single-phase cubic closest-packed structure of the ZVIN were dissolved after the influence

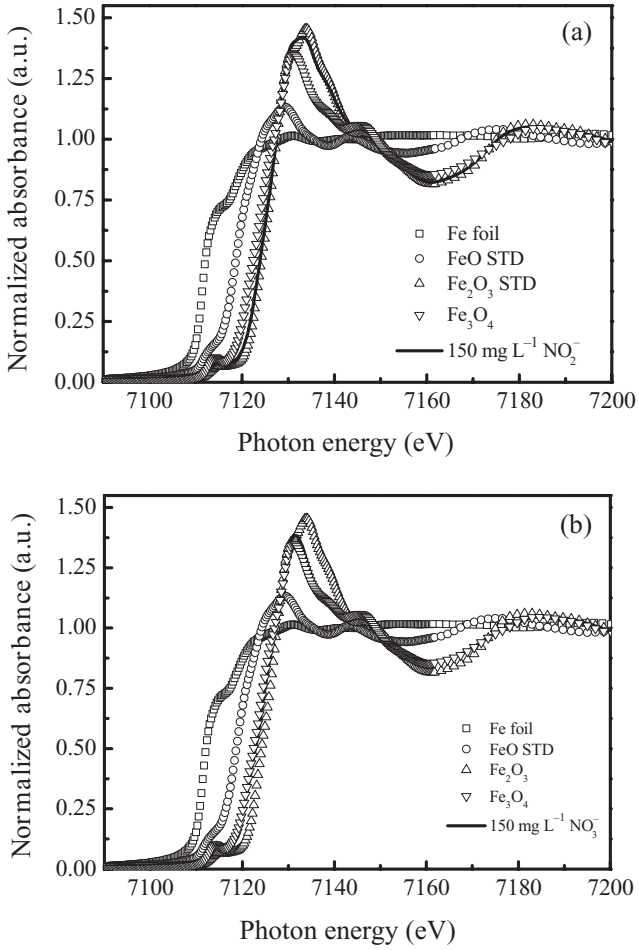


**Figure 6.** Fe K-edge XANES for the reduction of (a) $NO_2^-$ and (b) $NO_3^-$ solutions with the initial concentration of 150 mg $l^{-1}$.

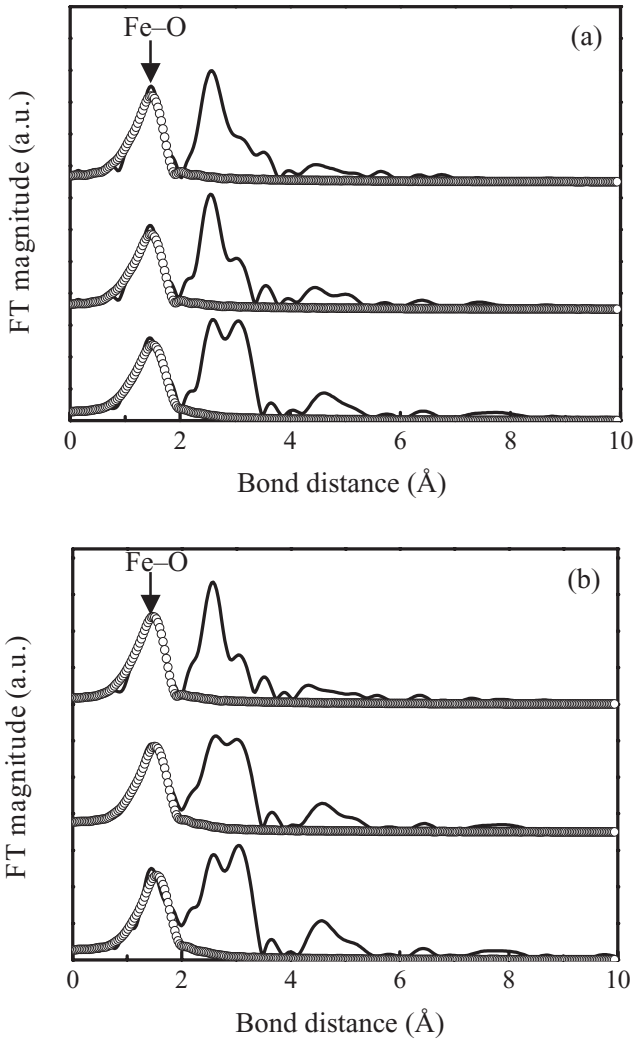


**Figure 7.** Fourier transform of Fe K-edge EXAFS for the reduction of (a) $NO_2^-$ and (b) $NO_3^-$ solutions with the initial concentrations of 150, 200, and 250 mg $l^{-1}$, respectively. The best fitting of the EXAFS spectra are expressed with the circle lines.

of nitrites or nitrates. The result suggests that the phase transformation in the iron corrosion be linked with the varying concentrations (e.g. 150, 200, and 250 mg $l^{-1}$) of nitrite or nitrate. In figure 5(a), XRD pattern collected at lower nitrite concentrations diminishes with the available ZVIN when forming the $Fe_2O_3$. Moreover, higher nitrite concentrations might be reduced rapidly on the ZVIN surface to form $Fe_3O_4$, thereby decreasing the intensity of the peak significantly. Nitrite concentration starting from 200 mg $l^{-1}$ was provided in surplus against Fe(II). The transformation is expected due to the Fe(III) is more readily stable. Figures 5(a) and (b) suggest that the quantitative relationship between nitrite to Fe(III) or Fe(II) be similar to the one between nitrate to Fe(III) on the ZVIN. Based on the XRD pattern analysis, it is found that the quantitative relationship between nitrite and Fe(III) or Fe(II) is similar to the one between nitrate and Fe(III) in the ZVIN study. The possible reason is due to a faster nitrite reduction on the surface of the ZVIN. In fact, the occurrence of the relatively faster nitrite reduction rate implies that the passivation of the ZVIN have a significant contribution to iron corrosion.

In order to more thoroughly examine the nature of the nitrite or nitrate species involved in chemical reduction on the ZVIN, the XANES and EXAFS spectra were also applied (figures 6 and 7). In fact, nitrite or nitrate is a strong oxidant and the production of nitrogen species depends on the form of iron corrosion, and availability of the adsorbed surface [19]. The XANES spectra may provide information of electronic configuration, stereochemistry and the oxidation states of Fe atoms in the ZVIN being investigated [20–23]. Figures 6(a) and (b) show that the pre-edge XANES spectra of Fe atom in these used ZVIN for the degradation of nitrite/nitrate solutions might exhibit an absorbance feature (Fe = 7115 eV) for the 1s to 3d transition, which was forbidden by the selection rule in the case of perfect octahedral symmetry. The sharp feature at 7134 eV, due to the dipole-allowed of 1s to $4p_{xy}$ electron transition, indicates the existence of Fe(III). The intensity of the 1s to $4p_{xy}$ transition was proportional to the population of Fe(III) of the used ZVIN in nitrate/nitrite solutions [20–23]. Similarly, due to the reduction of nitrate/nitrite species, a disappearing shoulder at 7109 eV and an intense feature at 7115 eV were attributed to the 1s to $4p_{xy}$ transition that indicate the existence of Fe species in ZVIN. Overall, nitrites were reduced directly on the ZVIN surface facilitating the reaction by dissolving away either Fe(II) or Fe(III). The

**Table 2.** Fine structural parameters of the fresh and used ZVIN for the treatment of 150, 200, and 250 mg $l^{-1}$ nitrite or nitrate solutions analyzed by EXAFS spectra.

| | Shell ($1^{st}$) | CN[a] | R (Å)[b] | $\Delta\sigma^2$ (Å$^2$)[c] |
|---|---|---|---|---|
| Fresh ZVI nanoparticle | | | | |
| | Fe–Fe | 9.66 | 2.25 | 0.0239 |
| Nitrite ($NO_2^-$) (mg $l^{-1}$) | | | | |
| 150 | Fe–O | 4.45 | 1.97 | 0.0122 |
| 200 | Fe–O | 4.21 | 1.98 | 0.0129 |
| 250 | Fe–O | 4.11 | 2.01 | 0.0132 |
| Nitrate-($NO_3^-$) (mg $l^{-1}$) | | | | |
| 150 | Fe–O | 4.45 | 1.99 | 0.0117 |
| 200 | Fe–O | 4.71 | 1.98 | 0.0124 |
| 250 | Fe–O | 4.88 | 1.97 | 0.0147 |

[a]CN: Coordination number.
[b]R: Bond distance.
[c] $\sigma$: Debye-Waller factor.

results also indicate the iron corrosion products could be a mixture of $Fe_2O_3$ and $Fe_3O_4$ after the reduction of nitrites. The corrosion might actually possess a stratified structure, shifting from an Fe(II)-rich, crystalline inner layer to an Fe(III)-rich, more amorphous outer layer. Oxygen might be the major atom coordinated to the two central Fe atoms in the used ZVIN. Therefore, nitrate and nitrite reduction significantly occurs due to the corrosion of the ZVIN to produce $Fe_2O_3$ and this is in the good agreements with our XANES spectra described in figures 6(a) and (b), respectively.

The EXAFS spectra indicate that the physicochemical properties of ZVIN used for the chemical reduction of nitrates and nitrates in figures 7(a) and (b). According to the EXAFS data shown in table 2 it can be observed that the used ZVIN have centers Fe atoms coordinated by Fe–O bonding. The fine structural parameters of the used ZVIN analyzed by the EXAFS data also suggested that the mirror-symmetrically ($D_d$) surrounded by Fe–O atoms in the different nitrite or nitrate concentrations. The EXAFS data also show that the increasing nitrite and nitrate concentration elevates the primarily coordinated Fe–O bond distance ranged from 1.97 to 2.01 Å and from 1.99 to 1.97 Å, respectively. The coordination numbers are much higher for nitrates reduction increased with concentration due to the requirement of higher oxidation state to the formation of nitrogen gases.

The chemical reduction of nitrites or nitrates on the ZVIN shows that the typical end product of this redox reaction might be an Fe(II) (i.e. FeO) or Fe(III) (i.e. $Fe_2O_3$). With the aid of previous findings, a substantial transformation of nitrite or nitrate to either nitrogen gas or ammonium is anticipated on the surface of ZVIN [9]. Fe(II) was often referred to as a stronger reductant [19]. However, Fe(II) was not readily capable to reduce nitrite due to the possible block via the presence of Fe(III). On the other hand, ZVIN is a more passive for the formation of Fe (III) rather than Fe(II) in a strong nitrite reduction pathway. Thus, the observation of iron corrosion evolved with time was affected by the concentrations of nitrites or nitrates.

## 4. Conclusions

The information generated in the present study could be valuable for understanding the postulated reaction pathway in a very complex adsorption and redox reaction process on the surface of the ZVIN corrosion. The FE-SEM microphotos of the ZVIN used for the treatment of nitrates or nitrites indicate that the ZVIN is nearly ball and ultrafine particles, which are on the order of 20–50 nm in size and strong magnetic force, are conducted for a narrow distribution. The reaction is successfully expressed as a pseudo first-order and the kinetic reaction orders are 0.86–0.95 for nitrite and 0.8–0.9 for nitrate based on different initial concentrations, respectively, when using the ZVIN. However, the ZVIN was oxidized and aggregated to form $Fe_2O_3$ nanoparticles in the chemical reduction process with respect to both nitrites and nitrates. With the XANES spectra, it was found that the nitrites or nitrates were reduced to $N_2$ while oxidizing the Fe(0) to $Fe_2O_3$ electrochemically. The EXAFS data also show that the used ZVIN have central Fe atoms coordinated by primarily the Fe–O with bond distances in a range from 1.97 to 1.99 Å, and the formation of Fe(III) species. The high reaction rates and significant removal efficiencies of toxic nitrate/nitrite contaminants suggest that the ZVIN might be a suitable and powerful material for an *in-situ* remediation of nitrate or nitrite contaminated in groundwater systems or waste streams.

## Acknowledgments

The financial supports of National Science Council (Contract No. NSC-94-2211-E-155-001) of Taiwan, ROC are gratefully acknowledged.

## References

[1] Walton G 1951 *Am. J. Public Health* **41** 986
[2] Cleemput O V and Samater A H 1996 *Fert. Res.* **45** 81
[3] Darbi A, Viraraghavan T, Butler R and Corkal D 2002 *Water* SA **28** 319
[4] Environmental Protection Administration (EPA) in Taiwan, Drinking Water Quality and Effluent Standards of Drinking Water, Groundwater, and Wastewater, Environmental Library, Taipei, Taiwan, 2007
[5] Chew C F and Zhang T C 1998 *Wat. Sci. Technol.* **38** 135
[6] Dash B P and Chaudhari S 2005 *Wat. Res.* **39** 4065
[7] Cooper D C, Picardal F W, Schimmelmann A and Coby A J 2003 *Appl. Environ. Microbial.* **69** 3517
[8] Huang C P, Wang H W and Chiu P C 1998 *Wat. Res.* **32** 2257
[9] Yang G C C and Lee H L 2005 *Wat. Res.* **39** 884
[10] Liou Y H, Lo S L, Lin C J, Kuan W H and Weng S C 2005 *J. Hazard. Mater.* B **126** 189
[11] Westerhoff P and James J 2003 *Wat. Res.* **37** 1818
[12] Chen S S, Hsu H D and Li C W 2004 *J. Nanoparticle Res.* **6** 639
[13] Chen Y M, Li C W and Chen S S 2005 *Chemosphere* **59** 753
[14] Hu H Y, Goto N and Fujie K 2001 *Wat. Res.* **35** 2789
[15] Choe S, Liljestrand H M and Khim J 2004 *Appl. Geochem.* **19** 335

[16] Alowitz M J and Scherer M M 2002 *Environ. Sci. Technol.* **36** 299
[17] Cheng F, Muftikian R, Fernando Q and Korte N 1997 *Chemosphere* **35** 2689
[18] Choe S, Chang Y Y, Hwang K Y and Khim J 2000 *Chemosphere* **41** 1307
[19] Huang Y H and Zhang T C 2006 *Chemosphere* **64** 937
[20] Conradson S D 1998 *Appl. Spectrosc.* **52** 252A
[21] Vlaic G, Andreatta D and Colavita P E 1998 *Catal. Today* **14** 261
[22] Lytle F W 1999 *J. Synchrotron Rad.* **6** 123
[23] Souza R F D, Simon L C and Alves M D C M 2003 *J. Catal.* **214** 165
[24] Thommes M, Koehn R and Froeba M 2000 *J. Phys. Chem.* B **104** 7932